

# Riemannian Optimization and Averaging Symmetric Positive Definite Matrices

Wen Huang<sup>1</sup>

with Xinru Yuan<sup>2</sup>, Kyle A. Gallivan<sup>2</sup>, and Pierre-Antoine Absil<sup>3</sup>

<sup>1</sup>Xiamen University, <sup>2</sup>Florida State University    <sup>3</sup>Université Catholique de Louvain

October 28, 2018  
Xiamen University

- Karcher mean computation on  $\mathcal{S}_{++}^n$
- Divergence-based means on  $\mathcal{S}_{++}^n$
- Riemannian  $L^1$  median computation on  $\mathcal{S}_{++}^n$
- Applications
- Conclusions

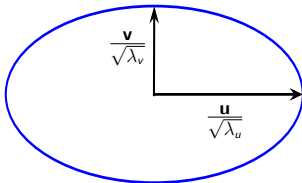
# Symmetric Positive Definite (SPD) Matrix

## Definition

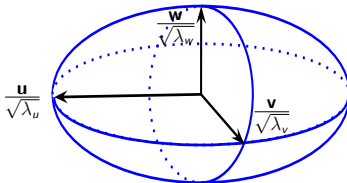
A symmetric matrix  $A$  is called **positive definite**  $A \succ 0$  iff all its eigenvalues are positive.

$$\mathcal{S}_{++}^n = \{A \in \mathbb{R}^{n \times n} : A = A^T, A \succ 0\}$$

2 × 2 SPD matrix



3 × 3 SPD matrix



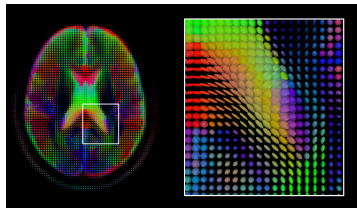
# Motivation of Averaging SPD Matrices

- Possible applications of SPD matrices

- Diffusion tensors in medical imaging [CSV12, FJ07, RTM07]
- Describing images and video [LWM13, SFD02, ASF<sup>+</sup>05, TPM06, HWSC15]

- Motivation of averaging SPD matrices

- denoising / interpolation
- clustering / classification





# Averaging Schemes: from Scalars to Matrices

Let  $A_1, \dots, A_K$  be SPD matrices.

- Generalized arithmetic mean:  $\frac{1}{K} \sum_{i=1}^K A_i$

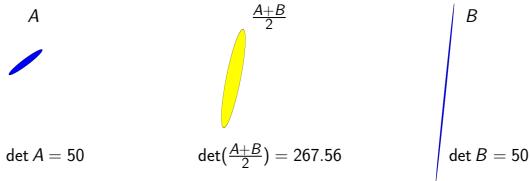
→ Not appropriate in many practical applications

# Averaging Schemes: from Scalars to Matrices

Let  $A_1, \dots, A_K$  be SPD matrices.

- Generalized arithmetic mean:  $\frac{1}{K} \sum_{i=1}^K A_i$

→ Not appropriate in many practical applications

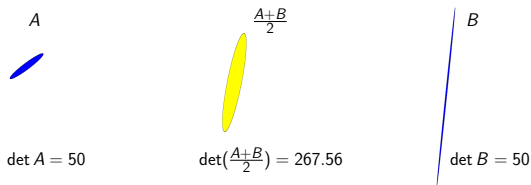


# Averaging Schemes: from Scalars to Matrices

Let  $A_1, \dots, A_K$  be SPD matrices.

- Generalized arithmetic mean:  $\frac{1}{K} \sum_{i=1}^K A_i$

→ Not appropriate in many practical applications



- Generalized geometric mean:  $(A_1 \cdots A_K)^{1/K}$

→ Not appropriate due to non-commutativity

→ How to define a matrix geometric mean?

# Desired Properties of a Matrix Geometric Mean

The desired properties are given in the ALM list<sup>1</sup>, some of which are:

- $G(A_{\pi(1)}, \dots, A_{\pi(K)}) = G(A_1, \dots, A_K)$  with  $\pi$  a permutation of  $(1, \dots, K)$
- if  $A_1, \dots, A_K$  commute, then  $G(A_1, \dots, A_K) = (A_1, \dots, A_K)^{1/K}$
- $G(A_1, \dots, A_K)^{-1} = G(A_1^{-1}, \dots, A_K^{-1})$
- $\det(G(A_1, \dots, A_K)) = (\det(A_1) \cdots \det(A_K))^{1/K}$

ALM list

---

<sup>1</sup>T. Ando, C.-K. Li, and R. Mathias, *Geometric means*, Linear Algebra and Its Applications, 385:305-334, 2004

# Geometric Mean of SPD Matrices

- A well-known mean on the manifold of SPD matrices is the **Karcher mean** [Kar77]:

$$G(A_1, \dots, A_K) = \arg \min_{X \in \mathcal{S}_{++}^n} \frac{1}{2K} \sum_{i=1}^K \delta^2(X, A_i), \quad (1)$$

where  $\delta(X, Y) = \|\log(X^{-1/2} Y X^{-1/2})\|_F$  is the geodesic distance under the affine-invariant metric

$$g(\eta_X, \xi_X) = \text{trace}(\eta_X X^{-1} \xi_X X^{-1})$$

- The Karcher mean defined in (1) satisfies all the geometric properties in the ALM list [LL11]

$$G(A_1, \dots, A_k) = \arg \min_{X \in \mathcal{S}_{++}^n} \frac{1}{2K} \sum_{i=1}^K \delta^2(X, A_i)$$

- Riemannian steepest descent [RA11] for Karcher mean
- Riemannian steepest descent, conjugate gradient, BFGS, and trust region Newton methods [JVV12] for general problems applied to Karch mean
- Richardson-like iteration [BI13] for Karcher mean
- Riemannian Barzilai-Borwein method with nonmonotone line search and the Karcher mean computation [IP17]

$$G(A_1, \dots, A_k) = \arg \min_{X \in \mathcal{S}_{++}^n} \frac{1}{2K} \sum_{i=1}^K \delta^2(X, A_i)$$

- Considered RTR-Newton-CG, RBFGS, RSD, RCG.
- First two considerably more complex per step than last two.
- RSD and RCG preferred.
- Higher rate of convergence for RBFGS (superlinear) and RTR-Newton-CG (quadratic) did not make up for extra complexity.
- Simpler first order methods recommended over a wide range of problems.

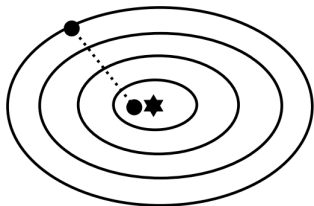
# Recent results on SPD Karcher mean computation

Based on Xinru Yuan, Wen Huang, Pierre-Antoine Absil, & Kyle A. Gallivan, *A Riemannian quasi-Newton method for computing the Karcher mean of symmetric positive definite matrices*, 2018.

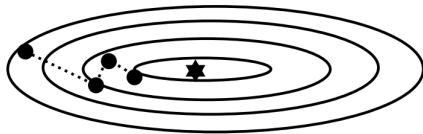


# Conditioning of the Objective Function

Hemstitching phenomenon  
for steepest descent



well-conditioned Hessian



ill-conditioned Hessian

- Small condition number  $\Rightarrow$  fast convergence
- Large condition number  $\Rightarrow$  slow convergence

# Conditioning of the Karcher Mean Objective Function

- **Riemannian metric:**

$$g_X(\xi, \eta) = \text{trace}(\xi X^{-1} \eta X^{-1})$$

**Condition number  $\kappa$  of Hessian at the minimizer  $\mu$ :**

- Hessian of Riemannian metric:

- $\kappa(H^R) \leq 1 + \frac{\ln(\max \kappa_i)}{2}$ ,  
where  $\kappa_i = \kappa(\mu^{-1/2} A_i \mu^{-1/2})$
- $\kappa(H^R) \leq 20$  if  
 $\max(\kappa_i) = 10^{16}$

# Conditioning of the Karcher Mean Objective Function

- **Riemannian metric:**

$$g_X(\xi, \eta) = \text{trace}(\xi X^{-1} \eta X^{-1})$$

- **Euclidean metric:**

$$g_X(\xi, \eta) = \text{trace}(\xi \eta)$$

**Condition number  $\kappa$  of Hessian at the minimizer  $\mu$ :**

- Hessian of Riemannian metric:

- $\kappa(H^R) \leq 1 + \frac{\ln(\max \kappa_i)}{2}$ ,  
where  $\kappa_i = \kappa(\mu^{-1/2} A_i \mu^{-1/2})$
- $\kappa(H^R) \leq 20$  if  
 $\max(\kappa_i) = 10^{16}$

- Hessian of Euclidean metric:

- $\frac{\kappa^2(\mu)}{\kappa(H^R)} \leq \kappa(H^E) \leq \kappa(H^R) \kappa^2(\mu)$
- $\kappa(H^E) \geq \kappa^2(\mu)/20$

# BFGS Quasi-Newton Algorithm: from Euclidean to Riemannian

- Update formula:

$$x_{k+1} = \underline{x_k + \alpha_k \eta_k}$$

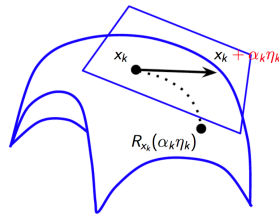
- Search direction:

$$\eta_k = -B_k^{-1} \text{grad } f(x_k)$$

- $B_k$  update:

$$B_{k+1} = B_k - \frac{B_k s_k s_k^T B_k}{s_k^T B_k s_k} + \frac{y_k y_k^T}{y_k^T s_k},$$

where  $s_k = \underline{x_{k+1} - x_k}$ , and  $y_k = \underline{\text{grad } f(x_{k+1}) - \text{grad } f(x_k)}$



Optimization on a Manifold

# BFGS Quasi-Newton Algorithm: from Euclidean to Riemannian

replace by  $R_{x_k}(\eta_k)$

Retraction

- Update formula:

$$x_{k+1} = \underline{x_k + \alpha_k \eta_k}$$

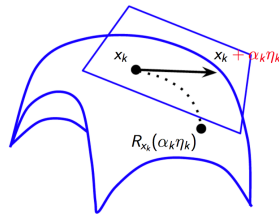
- Search direction:

$$\eta_k = -B_k^{-1} \text{grad } f(x_k)$$

- $B_k$  update:

$$B_{k+1} = B_k - \frac{B_k s_k s_k^T B_k}{s_k^T B_k s_k} + \frac{y_k y_k^T}{y_k^T s_k},$$

where  $s_k = \underline{x_{k+1} - x_k}$ , and  $y_k = \underline{\text{grad } f(x_{k+1}) - \text{grad } f(x_k)}$



Optimization on a Manifold

# BFGS Quasi-Newton Algorithm: from Euclidean to Riemannian

replace by  $R_{x_k}(\eta_k)$

Retraction

- Update formula:

$$x_{k+1} = x_k + \alpha_k \eta_k$$

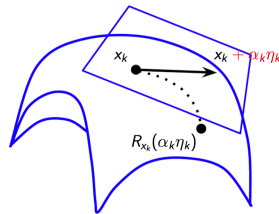
- Search direction:

$$\eta_k = -B_k^{-1} \text{grad } f(x_k)$$

- $B_k$  update:

$$B_{k+1} = B_k - \frac{B_k s_k s_k^T B_k}{s_k^T B_k s_k} + \frac{y_k y_k^T}{y_k^T s_k},$$

where  $s_k = x_{k+1} - x_k$ , and  $y_k = \text{grad } f(x_{k+1}) - \text{grad } f(x_k)$



Optimization on a Manifold

replaced by  $R_{x_k}^{-1}(x_{k+1})$

on different tangent spaces

Vector Trans.

# Riemannian BFGS (RBFGS) Algorithm

- Update formula:

$$x_{k+1} = R_{x_k}(\alpha_k \eta_k) \text{ with } \eta_k = -\mathcal{B}_k^{-1} \text{grad } f(x_k)$$

- $\mathcal{B}_k$  update [HGA15]:

$$\mathcal{B}_{k+1} = \tilde{\mathcal{B}}_k - \frac{\tilde{\mathcal{B}}_k s_k (\tilde{\mathcal{B}}_k s_k)^b}{(\tilde{\mathcal{B}}_k s_k)^b s_k} + \frac{y_k y_k^b}{y_k^b s_k},$$

where  $s_k = \mathcal{T}_{\alpha_k \eta_k} \alpha_k \eta_k$ ,  $y_k = \beta_k^{-1} \text{grad } f(x_{k+1}) - \mathcal{T}_{\alpha_k \eta_k} \text{grad } f(x_k)$ ,  
and  $\tilde{\mathcal{B}}_k = \mathcal{T}_{\alpha_k \eta_k} \circ \mathcal{B}_k \circ \mathcal{T}_{\alpha_k \eta_k}^{-1}$ .

- Stores and transports  $\mathcal{B}_k^{-1}$  as a dense matrix
- Requires excessive computation time and storage space for large-scale problem

# Limited-memory RBFGS (LRBFGS)

## Riemannian BFGS:

- Let  $\mathcal{H}_{k+1} = \mathcal{B}_{k+1}^{-1}$
- $\mathcal{H}_{k+1} = (\text{id} - \rho_k y_k s_k^b) \tilde{\mathcal{H}}_k (\text{id} - \rho_k y_k s_k^b) + \rho_k s_k s_k^b$   
where  $s_k = \mathcal{T}_{\alpha_k \eta_k} \alpha_k \eta_k$ ,  $y_k = \beta_k^{-1} \text{grad } f(x_{k+1}) - \mathcal{T}_{\alpha_k \eta_k} \text{grad } f(x_k)$ ,  
 $\rho_k = 1/g(y_k, s_k)$  and  $\tilde{\mathcal{H}}_k = \mathcal{T}_{\alpha_k \eta_k} \circ \mathcal{H}_k \circ \mathcal{T}_{\alpha_k \eta_k}^{-1}$

## Limited-memory Riemannian BFGS:

- Stores only the  $m$  most recent  $s_k$  and  $y_k$
- Transports these vectors to the new tangent space rather than  $\mathcal{H}_k$
- Computational and storage complexity depends upon  $m$



# Implementations

- Representations of tangent vectors
- Retraction
- Vector transport

# Implementations

- Representations of tangent vectors:  $T_X \mathcal{S}_{++}^n = \{S \in \mathbb{R}^{n \times n} | S = S^T\}$

- Extrinsic representation:  $n^2$ -dimensional vector

- **Intrinsic representation**:  $d$ -dimensional vector where  $d = n(n+1)/2$  Detail

- Retraction

- Vector transport

# Implementations

- Representations of tangent vectors:  $T_X \mathcal{S}_{++}^n = \{S \in \mathbb{R}^{n \times n} | S = S^T\}$ 
  - Extrinsic representation:  $n^2$ -dimensional vector
  - **Intrinsic representation**:  $d$ -dimensional vector where  $d = n(n+1)/2$  Detail
- Retraction
  - Exponential mapping:  $\text{Exp}_X(\xi) = X^{1/2} \exp(X^{-1/2} \xi X^{-1/2}) X^{1/2}$
- Vector transport
  - Parallel translation:  $\mathcal{T}_{p_\eta}(\xi) = Q \xi Q^T$ , with  $Q = X^{\frac{1}{2}} \exp(\frac{X^{-\frac{1}{2}} \eta X^{-\frac{1}{2}}}{2}) X^{-\frac{1}{2}}$

# Implementations

- Representations of tangent vectors:  $T_X \mathcal{S}_{++}^n = \{S \in \mathbb{R}^{n \times n} | S = S^T\}$

- Extrinsic representation:  $n^2$ -dimensional vector

- **Intrinsic representation**:  $d$ -dimensional vector where  $d = n(n+1)/2$  Detail

- Retraction

- Exponential mapping:  $\text{Exp}_X(\xi) = X^{1/2} \exp(X^{-1/2} \xi X^{-1/2}) X^{1/2}$

- **Second order approximation retraction [JVV12]:**

$$R_X(\xi) = X + \xi + \frac{1}{2} \xi X^{-1} \xi$$

- Vector transport

- Parallel translation:  $\mathcal{T}_{p_\eta}(\xi) = Q \xi Q^T$ , with  $Q = X^{\frac{1}{2}} \exp\left(\frac{X^{-\frac{1}{2}} \eta X^{-\frac{1}{2}}}{2}\right) X^{-\frac{1}{2}}$

- **Vector transport by parallelization [HAG15]: essentially an identity**

Parallelization

# Complexity Comparison for LRBFGS

## Extrinsic approach:

- Function
- Riemannian gradient
- Retraction
- Riemannian metric
- $(2m)$  times of vector transport

## Intrinsic approach:

- Function
- Riemannian gradient
- Retraction
- Reduces to Euclidean metric
- No explicit vector transport

## Complexity comparison:

- $f + \nabla f +$   
 $27n^3 + 12mn^2 +$   
 $2m \times \text{Vector transport cost}$

- $f + \nabla f +$   
 $22n^3/3 + 4mn^2$

# Problem Related Functions

- Cost function:

$$F(X) = \frac{1}{2K} \sum_{i=1}^K \text{dist}^2(A_i, X) = \frac{1}{2K} \sum_{i=1}^K \|\log(A_i^{-1/2} X A_i^{-1/2})\|_F^2$$

- Riemannian gradient:

$$\text{grad } F(X) = \frac{1}{K} \sum_{i=1}^K A_i^{1/2} \log(A_i^{-1/2} X A_i^{-1/2}) A_i^{-1/2} X^{1/2}$$

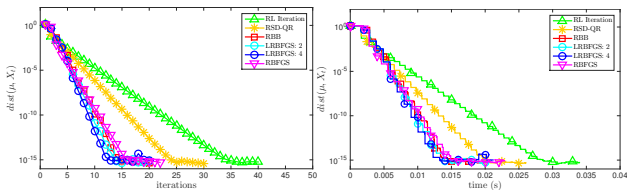
- Riemannian Hessian action on tangent vector:

$$\begin{aligned} \text{Hess } F(X)[\xi_X] &= \frac{1}{2K} \sum_{i=1}^K \xi_X \log(A_i^{-1} X) - \frac{1}{2K} \sum_{i=1}^K \log(X A_i^{-1}) \xi_X \\ &\quad + \frac{1}{K} \sum_{i=1}^K X D(\log)(A_i^{-1} X)[A_i^{-1} \xi_X] \end{aligned}$$

# Numerical Results: Comparison of Different Algorithms

$K = 100$ , size =  $3 \times 3$ ,  $d = 6$

- $1 \leq \kappa(A_i) \leq 200$



- $10^3 \leq \kappa(A_i) \leq 10^7$

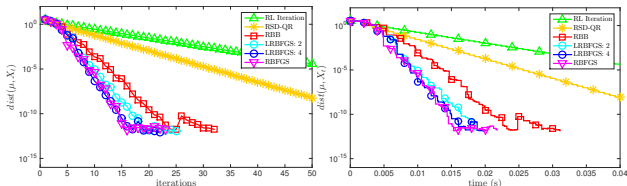
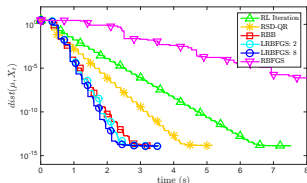
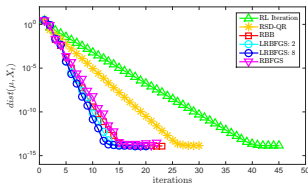


Figure: Evolution of averaged distance between current iterate and the exact Karcher mean with respect to time and iterations

# Numerical Results: Comparison of Different Algorithms

$K = 30$ , size =  $100 \times 100$ ,  $d = 5050$

•  $1 \leq \kappa(A_i) \leq 20$



•  $10^4 \leq \kappa(A_i) \leq 10^7$

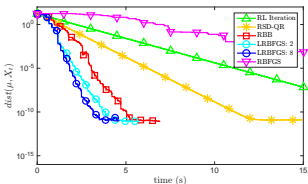
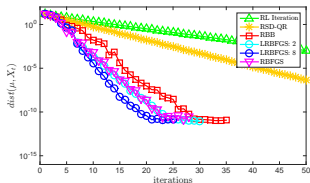
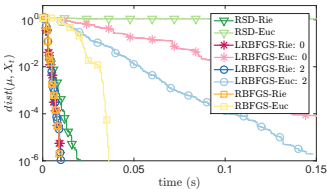
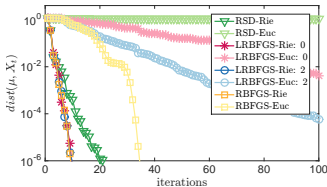


Figure: Evolution of averaged distance between current iterate and the exact Karcher mean with respect to time and iterations



# Numerical Results: Riemannian vs. Euclidean Metrics

- $K = 100$ ,  $n = 3$ , and  $1 \leq \kappa(A_i) \leq 10^6$ .



- $K = 30$ ,  $n = 100$ , and  $1 \leq \kappa(A_i) \leq 10^5$ .

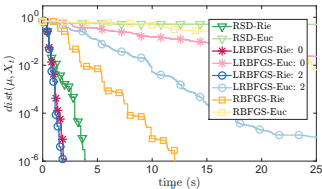
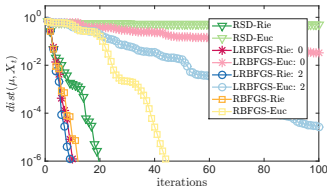


Figure: Evolution of averaged distance between current iterate and the exact Karcher mean with respect to time and iterations

- Karcher mean computation on  $\mathcal{S}_{++}^n$
- Divergence-based means on  $\mathcal{S}_{++}^n$
- Riemannian  $L^1$  median computation on  $\mathcal{S}_{++}^n$
- Applications
- Conclusions

- Karcher mean

$$K(A_1, \dots, A_K) = \arg \min_{X \in \mathcal{S}_{++}^n} \frac{1}{2K} \sum_{i=1}^K \delta^2(X, A_i), \quad (1)$$

where  $\delta(X, Y) = \|\log(X^{-1/2} Y X^{-1/2})\|_F$

- pros: holds desired properties
  - cons: high computational cost
- 
- Use [divergences](#) as alternatives to the geodesic distance due to their computational and empirical benefits
- 
- A [divergence](#) is like a distance except it lacks
    - triangle inequality
    - symmetry

# LogDet $\alpha$ -divergence and Associated Mean

The LogDet  $\alpha$ -divergence is defined as

$$G(A_1, \dots, A_k) = \arg \min_{X \in \mathcal{S}_{++}^n} \frac{1}{2K} \sum_{i=1}^K \delta_{\text{LD}, \alpha}^2(A_i, X), \quad (2)$$

where the **LogDet  $\alpha$ -divergence** on  $\mathcal{S}_{++}^n$  is given by

$$\delta_{\text{LD}, \alpha}^2(X, Y) = \frac{4}{1 - \alpha^2} \log \frac{\det(\frac{1-\alpha}{2}X + \frac{1+\alpha}{2}Y)}{\det(X)^{\frac{1-\alpha}{2}} \det(Y)^{\frac{1+\alpha}{2}}}$$

- The LogDet  $\alpha$ -divergence is asymmetric in general, except for  $\alpha = 0$
- (2) defines the **right mean**. The **left mean** can be defined in a similar way.

# Karcher Mean vs. LogDet $\alpha$ -divergence Mean

- Complexity comparison for problem-related operations

	function	gradient	total
LD $\alpha$ -div. mean	$\frac{2Kn^3}{3}$	$3Kn^3$	$\frac{11Kn^3}{3}$
Karcher mean	$18Kn^3$	$5Kn^3$	$23Kn^3$

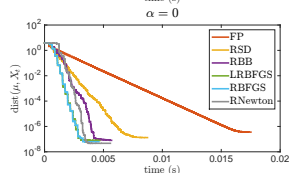
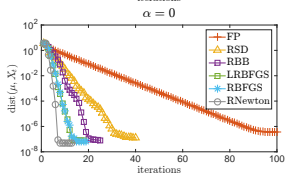
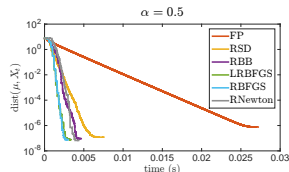
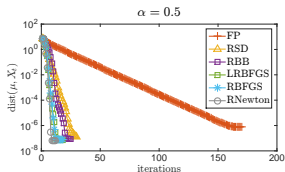
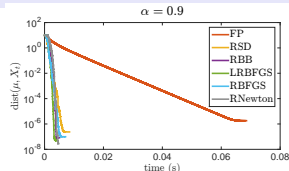
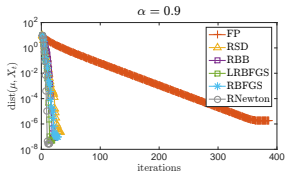
- Invariance properties

	scaling invariance	rotation invariance	congruence invariance	inversion invariance
LD $\alpha$ -div. mean	✓	✓	✓	✗
Karcher mean	✓	✓	✓	✓

# Numerical Experiment: Comparisons of Different Algorithms

$K = 100$ ,  $n = 3$ , and  $10 \leq \kappa(A_i) \leq 10^6$

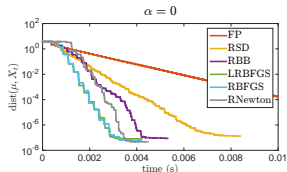
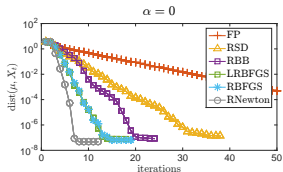
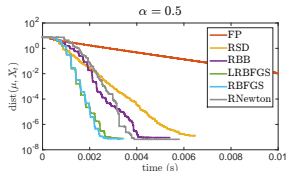
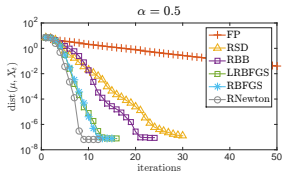
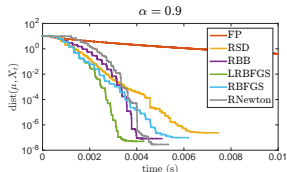
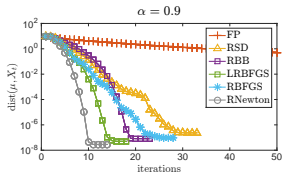
Fixed Point iteration<sup>2</sup>:  $\text{stepsize} = \frac{1 - \alpha}{2K}$



<sup>2</sup>Z. Chebbi and M. Moakher. Means of Hermitian positive-definite matrices based on the log-determinant -divergence function. Linear Algebra and its Applications, 436(7):1872C1889, 2012

# Numerical Experiment: Comparisons of Different Algorithms

- $K = 100$ ,  $n = 3$ , and  $10 \leq \kappa(A_i) \leq 10^6$



- Karcher mean computation on  $\mathcal{S}_{++}^n$
- Divergence-based means on  $\mathcal{S}_{++}^n$
- Riemannian  $L^1$  median computation on  $\mathcal{S}_{++}^n$
- Applications
- Conclusions



# Motivations

- The **mean** is sensitive to outliers
- The **median** is less sensitive to outliers

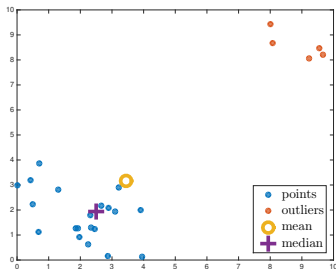


Figure: The geometric mean and median in  $\mathbb{R}^2$  space.

# Riemannian Median of SPD Matrices

The Riemannian median of a set of SPD matrices is defined as

$$M(A_1, \dots, A_K) = \arg \min_{X \in \mathcal{S}_{++}^n} \frac{1}{2K} \sum_{i=1}^K \delta(A_i, X),$$

where  $\delta$  is a distance or the square root of a divergence function

- The cost function is nonsmooth at  $X = A_i$
- If  $\delta$  is the geodesic distance, the median is unique

$$M(A_1, \dots, A_K) = \arg \min_{X \in \mathcal{S}_{++}^n} \frac{1}{2K} \sum_{i=1}^K \delta(A_i, X)$$

- Riemannian Weiszfeld's algorithm [FVJ09]
- Our approach: Riemannian quasi-Newton algorithms
  - Smooth RBFGS [HAG18]
  - Modified RBFGS [Hua12]
  - Nonsmooth RBFGS [HHY18]
  - Limited-memory versions of the above three [HAGH16]

# Numerical Results for $L^1$ Median Computation on $\mathcal{S}_{++}^n$ :

## Comparison of Different Algorithms

- $K = 100$ , size =  $3 \times 3$
- well-conditioned  $A_i$

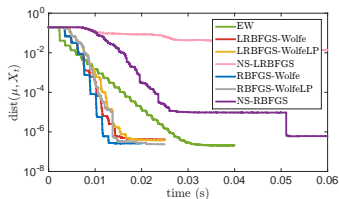
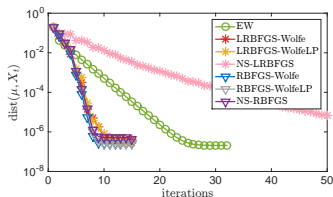


**Figure:** Evolution of averaged distance between current iterate and the exact Riemannian median with respect to time and iterations.

# Numerical Results for $L^1$ Median Computation on $\mathcal{S}_{++}^n$ :

## Comparison of Different Algorithms

- $K = 100$ , size =  $3 \times 3$
- well-conditioned  $A_i$  + 5% ill-conditioned outliers

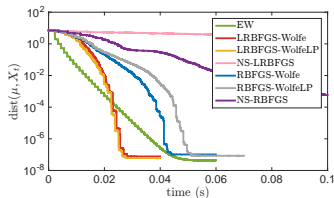
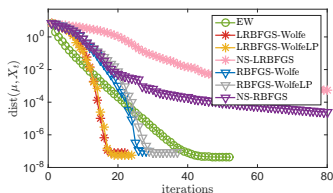


**Figure:** Evolution of averaged distance between current iterate and the exact Riemannian median with respect to time and iterations.

- Karcher mean computation on  $\mathcal{S}_{++}^n$
- Divergence-based means on  $\mathcal{S}_{++}^n$
- Riemannian  $L^1$  median computation on  $\mathcal{S}_{++}^n$
- Applications
  - Application I: Structure tensor image denoising
  - Application II: EEG classification based on the minimum distance to mean classifier
  - Application III: Image clustering
- Conclusions

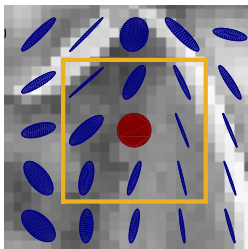
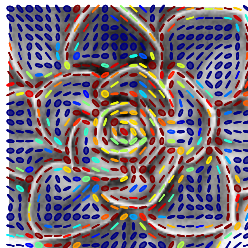
# Application: Structure Tensor Image Denoising

- A **structure tensor image** is a spatial structured matrix field

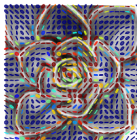
$$\mathcal{I} : \Omega \subset \mathbb{Z}^2 \rightarrow \mathcal{S}_{++}^n$$

- Noisy tensor images are simulated by replacing the pixel values by an outlier tensor with a given probability  $Pr$
- **Denoising** is done by averaging matrices in the neighborhood of each pixel
- Mean Riemannian Error:

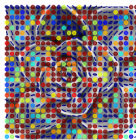
$$MRE = \frac{1}{\#\Omega} \sum_{(i,j) \in \Omega} \delta_R(\mathcal{I}_{i,j}, \tilde{\mathcal{I}}_{i,j})$$



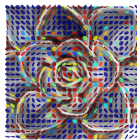
# Structure Tensor Image Denoising: $Pr = 0.1$



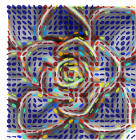
(g) Original image



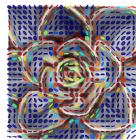
(h) A-mean



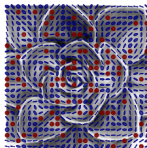
(i) K-mean



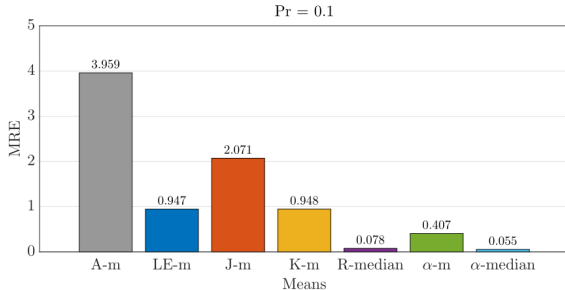
(j) R-median



(k)  $\alpha$ -mean



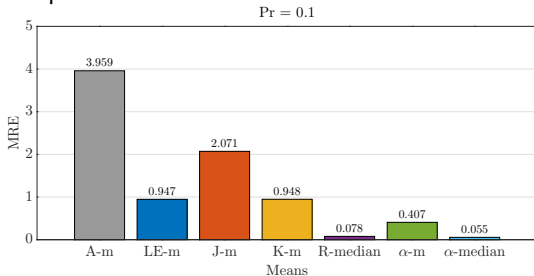
(l) Noisy image  
 $Pr = 0.1$



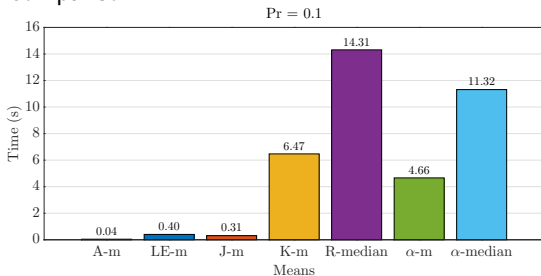


# Structure Tensor Image Denoising: MRE and Time

- MRE comparison



- Time comparison



# Application II: Electroencephalography (EEG) Classification

13 Hz



17 Hz



21 Hz

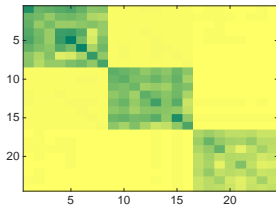


No led

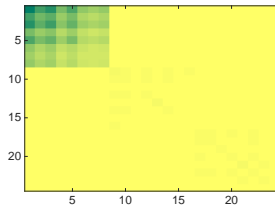
- The subject is either asked to focus on one specific blinking LED or a location without LED
- EEG system is used to record brain signals
- Covariance matrices of size  $24 \times 24$  are used to represent EEG recordings [KCB<sup>+</sup>15, MC17]

# EEG Classification: Examples of Covariance Matrices

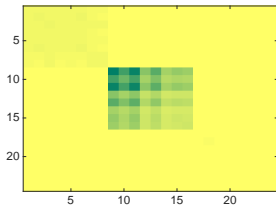
Resting Class



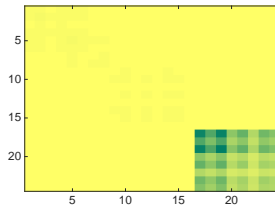
13 Hz Class



17 Hz Class

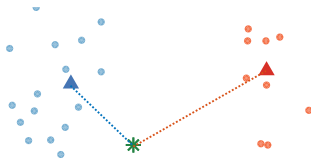


21 Hz Class



# EEG Classification: Minimum Distance to Mean classifier

**Goal:** classify new covariance matrix using Minimum Distance to Mean Classifier

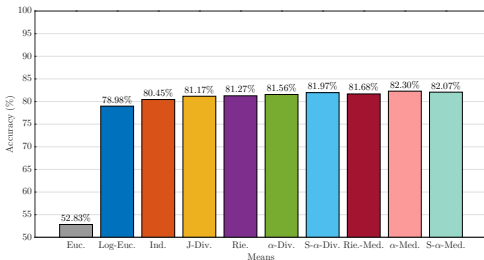


- For each class  $k = 1, \dots, K$ , compute the center  $\mu_k$  of the covariance matrices in the training set that belong to class  $k$
- Classify a new covariance matrix  $X$  according to

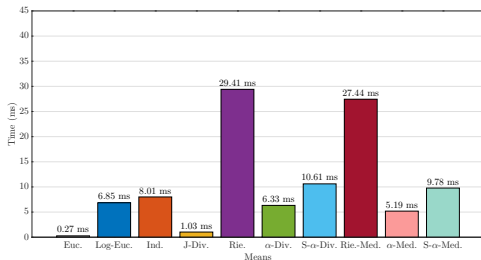
$$\hat{k} = \arg \min_{1 \leq k \leq K} \delta(X, \mu_k)$$

# EEG Classification: Accuracy and Computation Time

- Accuracy comparison

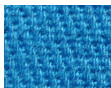


- Computation time comparison



# Application III: Image Clustering Using K-means Method

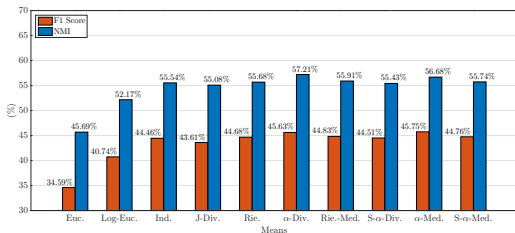
- The KTH-TIPS2 dataset [MFT<sup>+</sup>06]



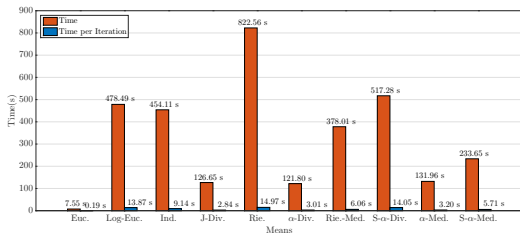
- 4752 samples, 11 categories, 432 samples per category
  - Region Covariance Matrices:  $23 \times 23$
- 
- Performance metrics to measure the **quality** of K-means clustering
    - F1-Score
    - Normalized mutual information (NMI)
- 
- Performance metrics to measure the **timing** of K-means clustering
    - Total computation time
    - Computation time per iteration

# Image Clustering: Comparison of Different K-means Variants

- Quality comparison



- Timing comparison



- Karcher mean computation on  $\mathcal{S}_{++}^n$
- Divergence-based means on  $\mathcal{S}_{++}^n$
- Riemannian  $L^1$  median computation on  $\mathcal{S}_{++}^n$
- Applications
- Conclusions



# Conclusions

- Investigate different averaging techniques for SPD matrices, including the computation of means and medians centers
- Use recent developments in Riemannian optimization to develop efficient and robust algorithms on  $\mathcal{S}_{++}^n$
- Provide empirical assessments and comparisons of the performance of considered Riemannian optimization algorithms and existing state-of-the-art algorithms
- Contribute a C++ toolbox for various averaging techniques (based on ROPTLIB)
- Evaluate the performance of different averaging techniques in applications

Thank you!



Ognjen Arandjelovic, Gregory Shakhnarovich, John Fisher, Roberto Cipolla, and Trevor Darrell.

Face recognition with image sets using manifold density divergence.  
In *Computer Vision and Pattern Recognition, 2005. CVPR 2005. IEEE Computer Society Conference on*, volume 1, pages 581–588.  
IEEE, 2005.



D. A. Bini and B. Iannazzo.

Computing the Karcher mean of symmetric positive definite matrices.

*Linear Algebra and its Applications*, 438(4):1700–1710, 2013.



Andrzej Cichocki, Sergio Cruces, and Shun-ichi Amari.

Log-determinant divergences revisited: Alpha-beta and gamma log-det divergences.

*Entropy*, 17(5):2988–3034, 2015.



Zeineb Chebbi and Maher Moakher.

Means of Hermitian positive-definite matrices based on the log-determinant  $\alpha$ -divergence function.

*Linear Algebra and its Applications*, 436(7):1872–1889, 2012.



Guang Cheng, Hesamoddin Salehian, and Baba Vemuri.

Efficient recursive algorithms for computing the mean diffusion tensor and applications to DTI segmentation.

*Computer Vision–ECCV 2012*, pages 390–401, 2012.



P. T. Fletcher and S. Joshi.

Riemannian geometry for the statistical analysis of diffusion tensor data.

*Signal Processing*, 87(2):250–262, 2007.



P Thomas Fletcher, Suresh Venkatasubramanian, and Sarang Joshi.

The geometric median on Riemannian manifolds with application to robust atlas estimation.

*NeuroImage*, 45(1):S143–S152, 2009.



Wen Huang, P-A Absil, and Kyle A Gallivan.  
A Riemannian symmetric rank-one trust-region method.  
*Mathematical Programming*, 150(2):179–216, 2015.



Wen Huang, P.-A. Absil, and K. A. Gallivan.  
A Riemannian BFGS Method without Differentiated Retraction for  
Nonconvex Optimization Problems.  
*SIAM Journal on Optimization*, 28(1):470–495, 2018.



Wen Huang, PA Absil, KA Gallivan, and Paul Hand.  
ROPTLIB: an object-oriented C++ library for optimization on  
Riemannian manifolds.  
Technical report, Technical Report FSU16-14, Florida State  
University, 2016.



Wen Huang, Kyle A Gallivan, and P-A Absil.  
A Broyden class of quasi-Newton methods for Riemannian  
optimization.  
*SIAM Journal on Optimization*, 25(3):1660–1685, 2015.



Syedehsomayeh Hosseini, Wen Huang, and Rohollah Yousefpour.  
Line search algorithms for locally Lipschitz functions on Riemannian manifolds.

*SIAM Journal on Optimization*, 28(1):596–619, 2018.



Wen Huang.

*Optimization algorithms on Riemannian manifolds with applications*.  
PhD thesis, Department of Mathematics, Florida State University,  
2012.



Zhiwu Huang, Ruiping Wang, Shiguang Shan, and Xilin Chen.  
Face recognition on large-scale video in the wild with hybrid  
Euclidean-and-Riemannian metric learning.

*Pattern Recognition*, 48(10):3113–3124, 2015.



Bruno Iannazzo and Margherita Porcelli.

The Riemannian Barzilai–Borwein method with nonmonotone line  
search and the matrix geometric mean computation.

*IMA Journal of Numerical Analysis*, 38(1):495–517, 2017.



B. Jeuris, R. Vandebril, and B. Vandereycken.

A survey and comparison of contemporary algorithms for computing the matrix geometric mean.

*Electronic Transactions on Numerical Analysis*, 39:379–402, 2012.



H. Karcher.

Riemannian center of mass and mollifier smoothing.

*Communications on Pure and Applied Mathematics*, 1977.



Emmanuel K Kalunga, Sylvain Chevallier, Quentin Barthélemy, Karim Djouani, Yskandar Hamam, and Eric Monacelli.

From Euclidean to Riemannian means: Information geometry for SSVEP classification.

In *International Conference on Networked Geometric Science of Information*, pages 595–604. Springer, 2015.



J. Lawson and Y. Lim.

Monotonic properties of the least squares mean.

*Mathematische Annalen*, 351(2):267–279, 2011.



Jiwen Lu, Gang Wang, and Pierre Moulin.

Image set classification using holistic multiple order statistics features and localized multi-kernel metric learning.

In *Proceedings of the IEEE International Conference on Computer Vision*, pages 329–336, 2013.



Estelle M Massart and Sylvain Chevallier.

Inductive means and sequences applied to online classification of EEG.

Technical report, ICTEAM Institute, Université Catholique de Louvain, 2017.



P Mallikarjuna, M Fritz, A Tavakoli Targhi, E Hayman, B Caputo, and JO Eklundh.

The KTH-TIPS and KTH-TIPS2 databases, 2006.





Q. Rentmeesters and P.-A. Absil.

Algorithm comparison for Karcher mean computation of rotation matrices and diffusion tensors.

In *19th European Signal Processing Conference*, pages 2229–2233, Aug 2011.



Y. Rathi, A. Tannenbaum, and O. Michailovich.

Segmenting images on the tensor manifold.

In *IEEE Conference on Computer Vision and Pattern Recognition*, pages 1–8, June 2007.



Gregory Shakhnarovich, John W Fisher, and Trevor Darrell.

Face recognition from long-term observations.

In *European Conference on Computer Vision*, pages 851–865. Springer, 2002.



Oncel Tuzel, Fatih Porikli, and Peter Meer.  
Region covariance: A fast descriptor for detection and classification.  
In *European conference on computer vision*, pages 589–600.  
Springer, 2006.



S. J. Wright and J. Nocedal.  
*Numerical optimization*.  
Springer New York, 2 edition, 2006.

# Intrinsic Representation of Tangent Vectors

- Tangent vector  $\eta_X \in T_X \mathcal{M}$  can be represented by its **intrinsic representation**, i.e., a  $d$ -dimensional vector of coordinates in a given basis of  $B_X$  of  $T_X \mathcal{M}$
- If  $B_X = \{b_1, \dots, b_d\}$ ,  $\eta_X = \alpha_1 b_1 + \dots + \alpha_d b_d$ , then  $\eta_X^d = B_X^b \eta_X$  and  $\eta_X^d = (\alpha_1, \dots, \alpha_d)^T$
- Reduces storage of tangent vectors and simplifies certain Riemannian objects if  $B_X$  is orthonormal and the coefficients  $\alpha_i$ 's are easy to compute

Go Back  $\leftrightarrow$

# Vector Transport by Parallelization

- **Vector transport by parallelization** is defined as  $\mathcal{T} = B_Y B_X^b$ , where  $B_Y$  and  $B_X$  are bases of  $T_Y \mathcal{M}$  and  $T_X \mathcal{X}$ , respectively
- If  $B_Y$  and  $B_X$  are orthonormal bases of  $T_Y \mathcal{M}$  and  $T_X \mathcal{M}$ , respectively, then the vector transport by parallelization is the identity
- Parallelization is an isometric vector transport

Go Back  $\leftarrow$

# Jointly Geodesically Convexity

## Definition

Let  $(\mathcal{M}, g)$  be a Riemannian manifold. A function  $f : \mathcal{M} \rightarrow \mathbb{R}$  is said to be **geodesically convex** if for any  $x, y \in \mathcal{M}$ , a geodesic  $\gamma$  such that  $\gamma(0) = x$  and  $\gamma(1) = y$ , and  $t \in [0, 1]$ , it holds that

$$f(\gamma(t)) \leq (1 - t)f(x) + tf(y) \quad (3)$$

## Definition

Let  $(\mathcal{M}, g)$  be a Riemannian manifold. A function  $f : \mathcal{M} \times \mathcal{M} \rightarrow \mathbb{R}$  is said to be **jointly geodesically convex** if for any  $x_1, x_2, y_1, y_2 \in \mathcal{M}$ , geodesics  $\gamma_x$  and  $\gamma_y$  such that  $\gamma_x(0) = x_1$ ,  $\gamma_x(1) = x_2$ ,  $\gamma_y(0) = y_1$  and  $\gamma_y(1) = y_2$ , and  $t \in [0, 1]$ , it holds that

$$f(\gamma_x(t), \gamma_y(t)) \leq (1 - t)f(x_1, y_1) + tf(x_2, y_2). \quad (4)$$

# Divergence Symmetrization

A divergence is asymmetric in general. There are two common ways to symmetrize a divergence [CCA15]:

- Type 1:

$$\delta_{S\phi}^2(X, Y) = \frac{1}{2}(\delta_{\phi}^2(X, Y) + \delta_{\phi}^2(Y, X)),$$

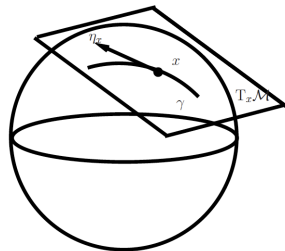
- Type 2:

$$\delta_{S\phi}^2(X, Y) = \frac{1}{2}(\delta_{\phi}^2(X, \frac{X+Y}{2}) + \delta_{\phi}^2(Y, \frac{X+Y}{2})).$$

- P1 Consistency with scalars. If  $A_1, \dots, A_K$  commute then  $G(A_1, \dots, A_K) = (A_1 \cdots A_K)^{1/K}$ .
- P2 Joint homogeneity.  $G(\alpha_1 A_1, \dots, \alpha_K A_K) = (\alpha_1 \cdots \alpha_K)^{1/K} G(A_1, \dots, A_K)$ .
- P3 Permutation invariance. For any permutation  $\pi(A_1, \dots, A_K)$  of  $(A_1, \dots, A_K)$ ,  $G(A_1, \dots, A_K) = G(\pi(A_1, \dots, A_K))$ .
- P4 Monotonicity. If  $A_i \geq B_i$  for all  $i$ , then  $G(A_1, \dots, A_K) \geq G(B_1, \dots, B_K)$  in the positive semidefinite ordering.
- P5 Continuity from above. If  $\{A_1^{(n)}\}, \dots, \{A_K^{(n)}\}$  are monotonic decreasing sequences (in the positive semidefinite ordering) converging to  $A_1, \dots, A_K$ , respectively, then  $G(A_1^{(n)}, \dots, A_K^{(n)})$  converges to  $G(A_1, \dots, A_K)$ .
- P6 Congruence invariance.  $G(S^T A_1 S, \dots, S^T A_K S) = S^T G(A_1, \dots, A_K) S$  for any invertible  $S$ .
- P7 Joint concavity.  $G(\lambda A_1 + (1 - \lambda) B_1, \dots, \lambda A_K + (1 - \lambda) B_K) \geq \lambda G(A_1, \dots, A_K) + (1 - \lambda) G(B_1, \dots, B_K)$ .
- P8 Invariance under inversion.  $G(A_1, \dots, A_K)^{-1} = G(A_1^{-1}, \dots, A_K^{-1})$ .
- P9 Determinant identity.  $\det G(A_1, \dots, A_K) = (\det A_1 \cdots \det A_K)^{1/K}$ .

# Tangent Vector

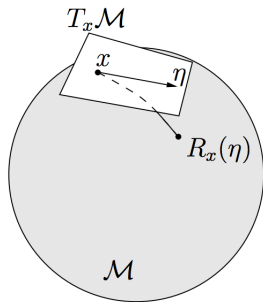
- **Definition:** The **tangent space**  $T_x \mathcal{M}$  is the vector space comprised of the tangent vectors at  $x \in \mathcal{M}$ . The **Riemannian metric** is an inner product on each tangent space.
- Tangent vectors can be represented by an **intrinsic representation**, which reduces the storage and simplifies certain Riemannian objects Intrinsic Representation





# Retraction

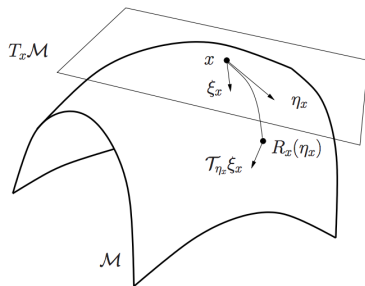
- Maps tangent vectors back to the manifold
- **Definition:** A **retraction** is a mapping  $R$  from  $T\mathcal{M}$  to  $\mathcal{M}$  satisfying the following:
  - $R$  is continuously differentiable
  - $R_x(0) = x$
  - $DR_x(0)(\eta) = \eta$



Euclidean	Riemannian
$x_{k+1} = x_k + \alpha_k \eta_k$	$x_{k+1} = R_{x_k}(\alpha_k \eta_k)$

# Vector Transport

- Some algorithms need to combine information on different tangent spaces to determine the next search direction
- **Vector transport**: transport a tangent vector from one tangent space to another
- $\mathcal{T}_{\eta_x} \xi_x$ , denotes transport of  $\xi_x$  to tangent space of  $R_x(\eta_x)$



Go Back  $\longleftrightarrow$

- Classical stepsize strategy in [WN06, (3.44)]

$$\alpha_{k+1} = \min\left\{1, 1.01 \cdot \frac{2(f(x_{k+1}) - f(x_k))}{g(\text{grad } f(x_{k+1}), -\text{grad } f(x_k))}\right\}$$

- Different versions of BB stepsizes

- $s_k = \mathcal{T}_{\alpha_k \eta_k}(\alpha_k \eta_k)$ ,  $y_k = \text{grad } f(x_{k+1}) - \mathcal{T}_{\alpha_k \eta_k}(\text{grad } f(x_k))$

- BB1:  $\alpha_{k+1} = g(s_k, s_k)/g(s_k, y_k)$

- BB2:  $\alpha_{k+1} = g(s_k, y_k)/g(y_k, y_k)$

- ABB<sub>min</sub>:

$$\alpha_{k+1} = \begin{cases} \min\{\alpha_j^{\text{BB2}} : j = \max(1, k - m_a), \dots, k\}, & \text{if } \alpha_{k+1}^{\text{BB2}}/\alpha_{k+1}^{\text{BB1}} < \tau \\ \alpha_{k+1}^{\text{BB1}}, & \text{otherwise} \end{cases}$$

- Classical stepsize strategy in [WN06, (3.44)]

$$\alpha_{k+1} = \min\left\{1, 1.01 \cdot \frac{2(f(x_{k+1}) - f(x_k))}{g(\text{grad } f(x_{k+1}), -\text{grad } f(x_k))}\right\}$$

- Different versions of BB stepsizes

- $s_k = \mathcal{T}_{\alpha_k \eta_k}(\alpha_k \eta_k)$ ,  $y_k = \text{grad } f(x_{k+1}) - \mathcal{T}_{\alpha_k \eta_k}(\text{grad } f(x_k))$

- BB1:  $\alpha_{k+1} = g(s_k, s_k)/g(s_k, y_k)$

- BB2:  $\alpha_{k+1} = g(s_k, y_k)/g(y_k, y_k)$

- ABB<sub>min</sub>:

$$\alpha_{k+1} = \begin{cases} \min\{\alpha_j^{\text{BB2}} : j = \max(1, k - m_a), \dots, k\}, & \text{if } \alpha_{k+1}^{\text{BB2}}/\alpha_{k+1}^{\text{BB1}} < \tau \\ \alpha_{k+1}^{\text{BB1}}, & \text{otherwise} \end{cases}$$

# LogDet $\alpha$ -divergence Mean: CM's Fixed-point Iteration

Chebbi and Moakher's fixed-point iteration [CM12] can be rewritten as

$$Y_{k+1} = \frac{1}{K} \sum_{i=1}^K \left( \frac{1-\alpha}{2} A_i + \frac{1+\alpha}{2} Y_k^{-1} \right)^{-1} \quad (1)$$

$$= Y_k - \frac{1-\alpha}{2K} \operatorname{grad} f(Y_k) \quad (2)$$

where  $\operatorname{grad} f(Y)$  denotes the Riemannian gradient of  $f(Y)$  and

$$f(Y) = \frac{4}{1-\alpha^2} \sum_{i=1}^K \left\{ \log \det \left( \frac{1-\alpha}{2} A_i + \frac{1+\alpha}{2} Y^{-1} \right) + \frac{1+\alpha}{2} \log \det Y \right\}$$

The fixed-point iteration is a Riemannian steepest descent using

- a constant stepsize  $(1-\alpha)/2K$
- Euclidean retraction  $R_X(\eta_X) = X + \eta_X$

# Background

Update for steepest descent:

$$\eta_k = -\alpha_k \operatorname{grad} f(x_k)$$

$$x_{k+1} = R_{x_k}(\eta_k)$$

- RSD:

- $\alpha_k$  is taken as the classical strategy in [WN06] Formula
- no use of second order information

- RBB:

- choose  $\alpha_k$  so that  $-\alpha_k \operatorname{grad} f(x_k)$  approximates  $-\operatorname{Hess} f(x_k)^{-1} \operatorname{grad} f(x_k)$   
i.e.,  $\alpha_k I$  approximates  $\operatorname{Hess} f(x_k)^{-1}$
- make use of second order information BB Stepsize

# Background

Update for steepest descent:

$$\begin{aligned}\eta_k &= -\alpha_k \operatorname{grad} f(x_k) \\ x_{k+1} &= R_{x_k}(\eta_k)\end{aligned}$$

- RSD:

- $\alpha_k$  is taken as the classical strategy in [WN06] Formula
- no use of second order information

- RBB:

- choose  $\alpha_k$  so that  $-\alpha_k \operatorname{grad} f(x_k)$  approximates  $-\operatorname{Hess} f(x_k)^{-1} \operatorname{grad} f(x_k)$   
i.e.,  $\alpha_k I$  approximates  $\operatorname{Hess} f(x_k)^{-1}$
- make use of second order information BB Stepsize

**Goal:** investigate the relationship between the BB stepsizes and the eigenvalues of the Riemannian Hessian of the objective function

**Goal:** investigate the relationship between the BB stepsizes and the eigenvalues of the Riemannian Hessian of the objective function

- Objective function used:  $f(X) = \frac{1}{2K} \sum_{i=1}^K \delta_{\text{LD},\alpha}^2(A_i, X)$
- $\{\lambda_1^{(k)}, \dots, \lambda_d^{(k)}\}$  are eigenvalues of the Riemannian Hessian of  $f$
- Compare  $1/\alpha_k$  and  $\{\lambda_1^{(k)}, \dots, \lambda_d^{(k)}\}$
- RBB is used with Armijo backtracking line search
- BB1, BB2,  $\text{ABB}_{\min}$  are compared BB Stepsize



# Numerical Experiment III: $\alpha = 0.5$

- $K = 200, 6 \times 6, d = 21$

